TISSUE ENGINEERING: Part A
Volume 25, Numbers 1 and 2, 2019

DOI: 10.1089/ten.tea.2017.0494

termis
Tissue Engineering
& Regenerative Medicine
International Society

SPECIAL FOCUS: RNA THERAPEUTICS FOR TISSUE ENGINEERING*

Aligned Nanofibrillar Scaffolds for Controlled Delivery of Modified mRNA

Tatiana S. Zaitseva, PhD,[1,**] Cynthia Alcazar, BS,[2,3,**] Maedeh Zamani, PhD,[2,4,**] Luqia Hou, PhD,[2–4] Steve Sawamura, BSc,[1] Eduard Yakubov, PhD,[5] Michael Hopkins, BS,[2,4] Y. Joseph Woo, MD,[2,4] Michael V. Paukshto, PhD, DSc,[1] and Ngan F. Huang, PhD[2–4]

RNA-based vector delivery is a promising gene therapy approach. Recent advances in chemical modification of mRNA structure to form modified mRNA (mmRNA or cmRNA or modRNA) have substantially improved their stability and translational efficiency within cells. However, mmRNA conventionally delivered in solution can be taken up nonspecifically or become cleared away prematurely, which markedly limits the potential benefit of mmRNA therapy. To address this limitation, we developed mmRNA-incorporated nanofibrillar scaffolds that could target spatially localized delivery and temporally controlled release of the mmRNA both *in vitro* and *in vivo*. To establish the efficacy of mmRNA therapy, mmRNA encoding reporter proteins such as green fluorescence protein or firefly luciferase (Fluc) was loaded into aligned nanofibrillar collagen scaffolds. The mmRNA was released from mmRNA-loaded scaffolds in a transient and temporally controlled manner and induced transfection of human fibroblasts in a dose-dependent manner. *In vitro* transfection was further verified using mmRNA encoding the angiogenic growth factor, hepatocyte growth factor (HGF). Finally, scaffold-based delivery of HGF mmRNA to the site of surgically induced muscle injury in mice resulted in significantly higher vascular regeneration after 14 days, compared to implantation of Fluc mmRNA-releasing scaffolds. After transfection with Fluc mmRNA-releasing scaffold *in vivo*, Fluc activity was detectable and localized to the muscle region, based on noninvasive bioluminescence imaging. Scaffold-based local mmRNA delivery as an off-the-shelf form of gene therapy has broad translatability for treating a wide range of diseases or injuries.

Keywords: modified mRNA, gene delivery, biomaterials, extracellular matrix, nanofibrillar scaffold

Introduction

Gene therapy is an attractive approach to modify cellular expression of key genes for therapeutic applications. Over the years, a number of approaches have been tested, including delivery of plasmids, viruses, and RNAi.[1–3] In particular, mRNA-based delivery has numerous advantages over conventional plasmid or viral-based technologies, including negligible risk of genome integration or insertional mutagenesis.[4] Recent advances in obtaining chemically modified mRNA (mmRNA) by incorporation of nucleotide analogs have shown substantially improved intracellular stability and translational efficiency while obviating innate immunity activation.[5] With these recent advances, mmRNA therapy has already shown promising therapeutic benefits to treat a number of diseases.[5–8] However, a major obstacle limiting the wider adoption of mmRNA for clinical use is its efficacy when delivered *in vivo*, which for soft tissue regeneration has predominantly been in solution.[9–11] Delivery of genetic material in solution shows dependency on injection technique[12] and variability in protein expression within specific target area.[10,13,14] Previous reports of intramyocardial injection of firefly luciferase (Fluc) mmRNA showed luciferase activity beyond the injection site in the heart,[14,15] and intramuscular injection of Fluc mmRNA resulted in systemic spread of the luciferase activity.[15]

[1]Fibralign Corporation, Union City, California.
[2]Stanford Cardiovascular Institute, Stanford, California.
[3]Veterans Affairs Palo Alto Health Care System, Palo Alto, California.
[4]Department of Cardiothoracic Surgery, Stanford University, Stanford, California.
[5]PhaRNA, LLC, Houston, Texas.
**These authors contributed equally to this work.

*This article is part of a special focus issue on RNA Therapeutics for Tissue Engineering.

Unlike delivery in solution, biomaterials-based delivery of genetic cargo targets cell populations located in the vicinity of the scaffold,[16] enables controlled release of the cargo,[17] and obviates premature clearance associated with solution-based delivery.[18] Scaffold-based delivery of mmRNA has been proven effective for bone regeneration.[19–21] However, to the best of our knowledge, this approach has not yet been used for the application of therapeutic angiogenesis and soft tissue regeneration. To stimulate muscle tissue regeneration by enhancing angiogenesis, we developed a technology using parallel-aligned nanofibrillar scaffolds for spatially controlled and transient release of mmRNA. With respect to genes that target neovessel formation, long-term uncontrolled expression of angiogenic transgenes has shown deleterious effects such as hemangioma and tumor formation.[22] Consequently, transient delivery of therapeutic mmRNA encoding angiogenic factors such as hepatocyte growth factor (HGF) may be suitable for inducing angiogenesis without long-term consequences.

Moreover, a three-dimensional scaffold intended for mmRNA delivery may also provide the structural framework for cellular recruitment and tissue formation in response to mmRNAs that encode angiogenic factors. Since physiological extracellular matrix (ECM) is often composed of nano- to microscale fibrillar networks,[23] we previously engineered aligned braided nanopatterned collagen scaffolds that induced cellular reorganization of the cytoskeleton along the direction of the nanofibrils[24–26] and improved cell survival.[27,28] Other studies further demonstrated a role of nanofibrillar cues in modulating cell function, stem cell differentiation, cellular reprogramming, and tissue morphogenesis,[29–31] suggesting that nanofibrillar scaffolds modulate basic cellular processes.

In this study, mmRNAs encoding green fluorescence protein (GFP), Fluc, or HGF were incorporated into aligned collagen nanofibrillar scaffolds. The transient release kinetics, dose-dependent effects and cellular transfection efficiency were quantitatively assessed. To demonstrate the efficacy of biomaterials (solid phase)-based mmRNA transfection *in vivo*, Fluc mmRNA-releasing scaffolds were implanted intramuscularly in a murine model, in which transfected cells were detected by bioluminescence imaging. The therapeutic benefit of HGF mmRNA-releasing scaffolds was demonstrated by enhanced vascular regeneration of the injured skeletal muscle. These studies demonstrate a novel approach to deliver mmRNA using biomaterials in muscle tissue, and the capability of mmRNA-loaded nanofibrillar scaffolds to localize mmRNA delivery and elicit therapeutic effect.

Materials and Methods

Fabrication and characterization of aligned nanofibrillar scaffolds

The aligned nanofibrillar collagen scaffolds were fabricated using shear-based fibrillogenesis technique[32,33] as described previously.[28] In brief, purified monomeric type I collagen solution was concentrated to reach a liquid crystal state[34–37] and then sheared onto a rigid surface,[38] creating thin film formed by parallel-aligned nanofibrils with 30–80 nm diameter.[38] To make three-dimensional thread-like scaffolds, the membranes were dissociated from the rigid surface into a free-standing film that self-assembled by liquid-air surface tension into the thread-like scaffold.[39] The scaffolds were then crosslinked by 1-ethyl-3-(3-dimethylaminopropyl)-1-carbodiimide hydrochloride (EDC) chemistry at 1 mg/mL and sterilized by e-beam per standard protocols (Fibralign). Scaffolds were assessed by routine scanning electron microscopy (SEM) as described previously.[40] For initial transfection studies, custom-made 96-well plates were prepared, which had bottoms of the well coated with thin parallel-aligned nanofibrillar collagen films (MuWells, San Diego).

Incorporation of mmRNA into aligned nanofibrillar scaffolds

mmRNA encoding GFP, human HGF, and Fluc were purchased from PhaRNA, LLC (Houston, TX). Each mmRNA was synthesized using predesigned and linearized plasmid templates integrated with extra-long stabilizing poly-A tail (175 nucleotides long) upstream from the site of linearization. The mmRNA was modified by the replacement of uridine with 5-methoxyuridine, and posttranscriptional enzymatic incorporation of Cap1 structure. After the production of the nanofibrillar scaffolds (0.3 mm thick), they were cut into 5-mm long samples, and mmRNA was loaded into the 5-mm scaffold along with Lipofectamine MessengerMax transfection agent (Invitrogen, Carlsbad, CA). The mmRNA-incorporated scaffold was then freeze-dried to promote infiltration of the mmRNA into the scaffold. For *in vitro* studies, a range of mmRNA loads (90–450 ng) was loaded into the scaffolds. For *in vivo* studies, 20 μg of Fluc was loaded into each scaffold.

Kinetics of mmRNA release in vitro

The kinetics of GFP and HGF mmRNA release were quantitatively assessed using the Quant-iT RiboGreen Quantification Kit (Thermo Fisher Scientific) according to the manufacturer's instructions. The mmRNA-loaded scaffolds were incubated in 100 μL buffer containing 10 mM Tris-HCl and 1 mM EDTA (TE buffer, pH 7.5). At specified time points, the TE buffer was removed for quantification by Ribogreen assay, and replaced with fresh TE buffer. After 14 days, the scaffolds were digested with proteinase K, and the mmRNA released from the scaffolds was quantified as described above to obtain the total recovered mmRNA per scaffold ($n = 3$).

Transfection with GFP and HGF mmRNA in vitro

Human fibroblasts (SCRC1041, ATCC, passages 5–10) were expanded in Dulbecco's modified Eagles medium with 10% fetal bovine serum and 1% penicillin/streptomycin. For direct transfection, fibroblasts (10^4) were seeded into 96-well plates, either standard tissue culture-treated or those having parallel-aligned nanofibrillar collagen film (the same initial material as used in fabrication of the thread-like scaffold) at the bottom of the well ($n = 3$). On day 1 after seeding, fibroblasts were transfected with GFP or HGF mmRNA at 12.5–150 ng RNA per well using Lipofectamine Messenger Max (Invitrogen). For solid phase transfection on scaffold, fibroblasts (10^5) were seeded into mmRNA-loaded scaffolds placed into 96-well ultralow attachment plate for 2 h. Then, the media with unattached cells were removed and replaced with fresh media. Cells on scaffolds were cultured for indicated time intervals ($n = 3$). For HGF

mmRNA-transfected cells, aliquots of media were removed periodically for analysis of secreted HGF protein and replaced with fresh media.

Intravital fluorescence imaging and immunocytochemistry

For cells transfected with GFP-mmRNA directly, on day 1 after transfection, cells were fixed in 4% paraformaldehyde (Fisher Scientific), permeabilized in 0.1% Triton-X-100 (Sigma), and stained with Hoechst 33342. For cells transfected with HGF mmRNA directly, cells were fixed and permeabilized as described above, and then stained with HGF antibody (mab694, R&D Systems) followed by Alexa Fluor 594 secondary antibody (Invitrogen) For each condition, three wells were analyzed, with three fluorescence microscopy images taken for each well, and the percentage of GFP^+ and HGF^+ cells was quantified as a ratio of positive cell count to total nuclei count. For GFP-mmRNA-transfected cells on scaffold, live fluorescence images were taken on day 1 or later after transfection, following fixation as described above and staining with GFP antibody (Fisher Scientific). For HGF-mmRNA transfected cells on scaffold, the staining was performed as described above. Images were acquired using a Leica DM IRB inverted fluorescence microscope (Leica Microsystems) equipped with Infinity 3 digital camera and Infinity Analyze software (Luminera corp.).

Immunoblotting and enzyme-linked immunosorbent assay

For analysis of GFP expression by immunoblotting, transfected cells grown in 96-well plates or on scaffolds were lysed at specified time points in RIPA buffer (Thermo Fisher Scientific) containing protease and phosphatase inhibitors. Protein concentration was determined by the BCA Protein Quantification Assay Kit (Pierce). Lysate samples adjusted to equal protein concentration were analyzed for GFP expression with anti-GFP antibody (Novus Biologicals) using automated immunoblotting assay (Wes, Protein Simple). GFP expression was normalized to β-actin (Sigma) expression ($n=3$). In addition, HGF concentration in media samples was measured by HGF ELISA kit (R&D Systems) following manufacturer's instructions ($n=4$).

Cellular transfection with mmRNA-releasing scaffolds transplanted in two murine muscle injury models

All animal experiments were performed with approval by the Institutional Animal Care and Use Committee at the Veterans Affairs Palo Alto Healthcare System. Male C57/BL mice (8–10 weeks old) were anesthetized with 2% isoflurane, and a longitudinal partial incision (10 mm long × 1–1.5 mm deep) was made to the tibialis anterior (TA) muscle. In the first injury model, nanofibrillar scaffolds loaded with 20 μg Fluc mmRNA and lipofectamine (10 mm × 1–1.5 mm) were directly implanted into the TA muscle ($n=4$, Supplementary Fig. S1; Supplementary Data are available online at www.liebertpub.com/tea). In the second model, 20% of the muscle was ablated, followed by transplantation of the scaffold into the void space ($n=4$, Supplementary Fig. S2).[41] The muscle and skin were subsequently sutured closed using 9–0 sutures (Ethicon). Efficiency of *in vivo* transfection was assessed by bioluminescence imaging, in which the delivery of D-luciferin into Fluc-expressing cells catalyzes the release of photons that can be detected using a bioluminescence detection system. For up to 9 days after implantation, animals were injected intraperitoneally with D-luciferin (150 μg/mL), and bioluminescence imaging was performed with an IVIS imaging system (IVIS-200, Xenogen Corp.). Data were acquired with Living Image software (Xenogen Corp.) and expressed in units of average radiance ($p/s/cm^2/sr$).

To fluorescently detect transfected cells *in vivo,* an additional study was performed, in which nanofibrillar scaffolds loaded with 20 μg GFP mmRNA and lipofectamine (10 mm × 1–1.5 mm) were implanted in the first injury model for explantation after 24 h. After 24 h, the muscle was cryosectioned and then imaged by confocal microscopy for GFP expression. In addition, a GFP antibody directly conjugated to Alexa Fluor 594 (Fisher Scientific) was used to confirm colocalization of GFP expression.

Therapeutic angiogenesis after implantation of HGF mmRNA-releasing scaffold in murine muscle injury model

In a separate experiment, male C57/BL mice (8–10 weeks old) were anesthetized with 2% isoflurane, and ablation of the TA muscle was performed as described above. The mmRNA-releasing scaffolds encoding for either HGF or Fluc were implanted into the void space, followed by suture closure of the wound site ($n=4$). After 14 days, the TA muscle was explanted, and embedded in OCT embedding media for cryosectioning of transverse tissue sections. Histological quantification of capillary density was performed by immunofluorescence staining for endothelial marker, CD31 (R&D Systems). Four nonoverlapping images (500 × 500 μm) from transverse cryosections for each animal ($n=4$ each group) were taken within 500 μm from the transplanted scaffolds using a fluorescence microscope (Keyence). The number of vessels was counted and expressed in the form of capillary density (# CD31 vessels/mm^2) as described previously.[40,42]

Statistical analysis

All data are shown as mean ± standard deviation. Statistical comparisons between two groups were quantified by an unpaired *t*-test. For comparisons of three or more groups, analysis of variance with Holm's adjustment for multiple comparisons was used. Statistical significance was accepted at $p<0.05$.

Results

Characterization of nanofibrillar scaffolds

Aligned nanofibrillar collagen scaffolds were fabricated by shear-based fibrillogenesis to form aligned nanofibrillar sheets, followed by self-assembly of the sheets to form thread-like scaffolds (Fig. 1A).[1] The aligned scaffolds were further crosslinked with EDC chemistry to modulate the degradation of the scaffold. Based on SEM, the thread-like scaffolds were structurally characterized by parallel-aligned nanofibrillar organization (Fig. 1B, C) with individual fibril diameters of ~30–80 nm.

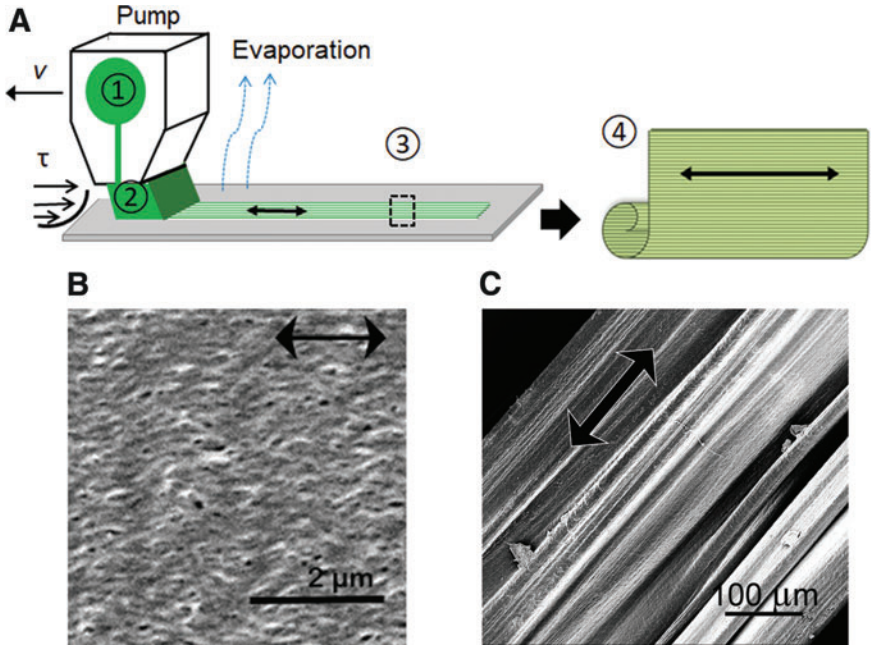

FIG. 1. Characterization of aligned nanofibrillar scaffold. **(A)** The schematic shows the shear-based fabrication of collagen film, and subsequent delamination to form a free standing 3D scaffold as follows: (1) loading collagen material into the applicator; (2) shearing the loaded material onto support; (3) collagen film drying on the support; (4) conversion of the collagen film (detached from the support) into thread. **(B, C)** Scanning electron microscopy images show the nanofibrillar organization of the collagen film **(B)** and surface structure of 3D collagen scaffold. Scale bar: 2 μm **(B)**, 100 μm **(C)**. 3D, three-dimensional. Color images available online at www.liebertpub.com/tea

Transfection of fibroblasts with mmRNA on aligned collagen film

To confirm the ability of cells to become transfected by mmRNA on collagen biomaterial, the efficiency of transfection using 100 ng GFP or HGF mmRNA was quantified for cells seeded on TC plastic and cells seeded on aligned collagen film. GFP- or HGF- positive cells were counted after acquisition of immunofluorescence images, and the numbers were normalized to the respective nuclei counts. Fibroblasts grown on aligned collagen film demonstrated a distinct alignment along the collagen fibrils and a visibly higher fluorescence intensity compared with those cultured on TC (Fig. 2A). Quantification of transfection efficiency (Fig. 2B) showed that the percentage of GFP-positive cells was significantly higher for cells cultured on aligned collagen film (73.3% ± 9.5%) compared with those grown on TC plates (36.2% ± 9.6%). Similarly, HGF-positive cells were more abundant when HGF mmRNA was introduced to cells cultured on aligned collagen film (75.8% ± 7.8%) compared with those grown on TC plates (42.8% ± 11.5%).

Release of GFP mmRNA from nanofibrillar scaffolds

Next, scaffolds were loaded with a fivefold range of mmRNA (90–450 ng), and mmRNA released in TE buffer was then quantified using RiboGreen assay. The kinetics of GFP mmRNA release over the course of 14 days (Fig 3A) reflects the highest load of mmRNA (450 ng; 5×) having the largest relative burst of mmRNA over 40% ± 4% during the first day, whereas the scaffold with the lowest load mmRNA (90 ng; 1×) had a significantly lower initial burst after day 1 (7% ± 1%). All scaffolds, regardless of the amount of loaded mmRNA, demonstrated an initial burst for the first day, followed by a much slower rate of release for the remainder of 14 days. At the end of 14 days, the mmRNA remaining in the scaffold was extracted by proteolytic degradation of the scaffolds with proteinase K. Further quantification of the cumulative recoverable mmRNA either released into solution or remaining in the scaffold showed that the total amount of detectable mmRNA ranged from 4% ± 1% for the 1× formulation to 15% ± 1% for the 5× formulation, suggesting only partial recovery of the loaded mmRNA.

Quantification of transfection on GFP mmRNA-loaded scaffold

After characterizing the release kinetics of mmRNA from scaffolds, the scaffold loaded with fivefold range of mmRNA (1× = 90, 3× = 270, and 5× = 450 ng) were seeded with human fibroblasts. On day 1 after seeding/transfection, life fluorescence imaging revealed GFP-positive cells aligned along the scaffold axis, with less positive cells on 1×-loaded scaffold and more GFP-positive cells on the 3× and 5× loaded scaffolds (Fig. 3B). To substantiate these results, we further analyzed GFP based on immunoblotting, in which the dose dependency of GFP mmRNA loading correlates to the percentage of GFP-positive cells as well as GFP protein abundance by immunoblotting (Supplementary Fig. S3). Immunoblot quantification of GFP expression in cell lysates obtained on day 1 after transfection by immunoblotting showed a clear dose dependency (Fig. 3C, Supplementary Fig. S4). Furthermore, temporal kinetics of GFP expression in fibroblasts seeded on 1×- and 5×-loaded scaffold showed that fibroblasts transfected on scaffolds with the highest load had the expression maintained through day 5 of culture, while those seeded/transfected on low-load scaffolds had lower and shorter GFP expression (Fig. 3D, Supplementary Fig. S4).

Verification of mmRNA release and transfection for HGF mmRNA-loaded scaffold

Based on the data demonstrating that a 450-ng GFP mmRNA load into scaffold provides for reliable transfection

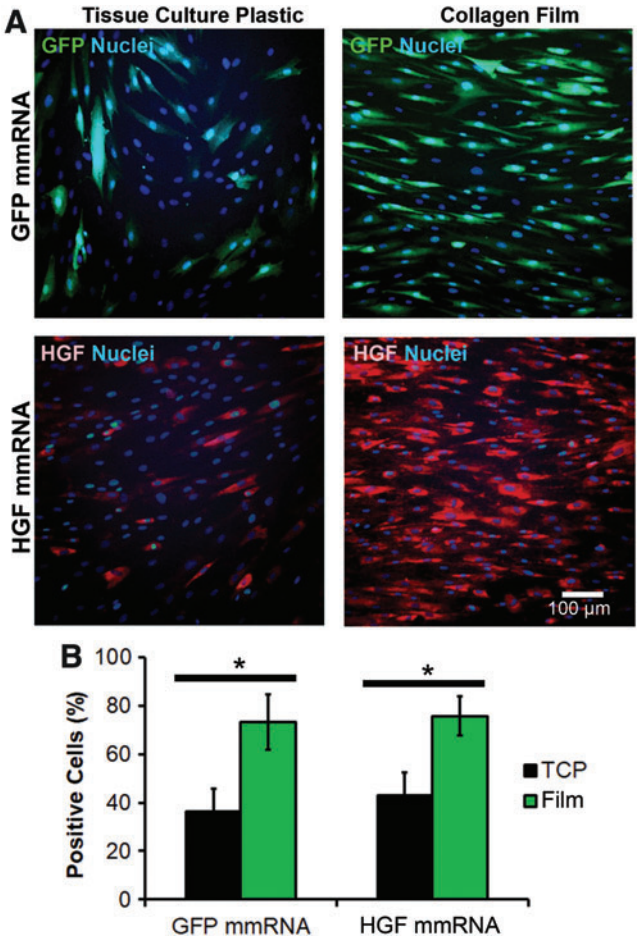

FIG. 2. Transfection efficiency of GFP and HGF mmRNA in human fibroblasts seeded on aligned nanofibrillar collagen film and TCP. Cells seeded on TCP or on collagen film were transfected for 1 day with 100 ng mmRNA added directly into the media. **(A)** Fluorescence microscopy images of GFP- and HGF-positive cells on TCP and aligned collagen film. **(B)** Quantification of the GFP- or HGF-positive cells. Percentage of the positive cells represents the ratio of positive cell count to nuclei count ($n=3$). *Statistically significant comparison ($p<0.05$). Scale bar: 100 μm. TCP, tissue culture plastic; HGF, hepatocyte growth factor; GFP, green fluorescence protein. Color images available online at www.liebertpub.com/tea

of fibroblasts and sustainable GFP expression, a set of scaffolds were loaded with a similar amount of HGF mmRNA. These HGF mmRNA-loaded scaffolds showed an average load recovery of 48.8% ± 10.7% and demonstrated an mmRNA release profile comparable to the GFP mmRNA-loaded scaffold (Fig. 4A). HGF-expressing cells aligned on scaffold 1 day after transfection were observed after staining with HGF antibodies (Fig. 4B). The concentration of HGF protein released into media by fibroblasts seeded and then transfected on HGF mmRNA-loaded scaffolds was measured by HGF ELISA. The results show that HGF concentration was sustained for at least 15 days (Fig. 4C). In contrast, the levels of HGF released into media from control scaffolds with no mmRNA load were significantly lower, with the highest values at 383 pg/mL (Supplementary Table S1, vs. 6936 pg/mL for the HGF mmRNA-loaded scaffolds), suggesting that the detected HGF was predominantly derived from exogenous HGF.

Cellular transfection with Fluc or GFP mmRNA-releasing scaffolds in murine intramuscular transplantation models

To verify these findings from *in vitro* studies, transfection efficiency was further assessed *in vivo*. Based on studies suggesting that mmRNA loading suitable for *in vivo* transfection range between 10 and 100 μg[11] aligned scaffolds loaded with Fluc mmRNA (20 μg) were transplanted into the murine TA muscle after a partial incision into the muscle (Supplementary Fig. S1). Bioluminescence detection of Fluc protein expression *in vivo* demonstrated a positive signal as early as 3 h after transplantation, followed by a peak in signal after day 1 and a gradual loss of Fluc signal within 7 days (Fig. 5A, B). The localized bioluminescence signal indicated that the transfected cells signal was primarily localized to the site of implantation in the TA muscle. To verify cellular transfection, in separate experiments the TA muscle of mice were intramuscularly implanted with GFP mmRNA-releasing scaffolds, and the muscle tissue was explanted after 24 h to coincide with peak of transfection. Fluorescence imaging of GFP revealed the presence of transfected muscle cells (Fig. 5C). These results were further confirmed by the use of fluorescently tagged GFP antibody, showing colocalization of the fluorescently tagged GFP antibody to direct GFP fluorescence in the muscle tissue (Supplementary Figs. S5 and S6).

Next, toward applying mmRNA-releasing scaffolds for treatment of muscle injuries, we implanted Fluc-mmRNA-releasing scaffolds into the ablated TA muscle after surgically removing 20% of the muscle. The scaffolds filled the void space (Supplementary Fig. S2). Quantification of bioluminescence imaging similarly demonstrated a peak signal on day 1 localized to the site of implantation (Fig. 6).

We further evaluated the therapeutic potential of mmRNA-releasing scaffold for delivery of the angiogenic growth factor, HGF, into the site of the ablated TA muscle. Two weeks after scaffold implantation, a significantly higher capillary density ($610 \pm 90/mm^2$) was induced by the HGF mmRNA-releasing scaffolds than by control Fluc-mmRNA-releasing scaffolds ($460 \pm 90/mm^2$), based on quantification of immunofluorescence staining for endothelial marker CD31 (Fig. 7). Together, these studies substantiate the *in vitro* findings that mmRNA can be successfully delivered from scaffolds and demonstrate an *in vivo* functional effect of therapeutic angiogenesis in a clinically relevant injury model.

Discussion

In recent years, mmRNA-based therapy has become a promising approach due to the negligible risk of mmRNA integration into the genome, low immunogenicity, transient mode of expression, natural biodegradation pathways, and efficiency of translation of the encoded therapeutic protein directly by translational machinery of mammalian cells. In previous studies, it has been demonstrated that translational rate of *in vitro* synthesized mRNA (IVT-RNA) depends on its transfection efficiency, which in turn directly correlates with overall IVT-mRNA toxicity.[43,44] Independently, it has

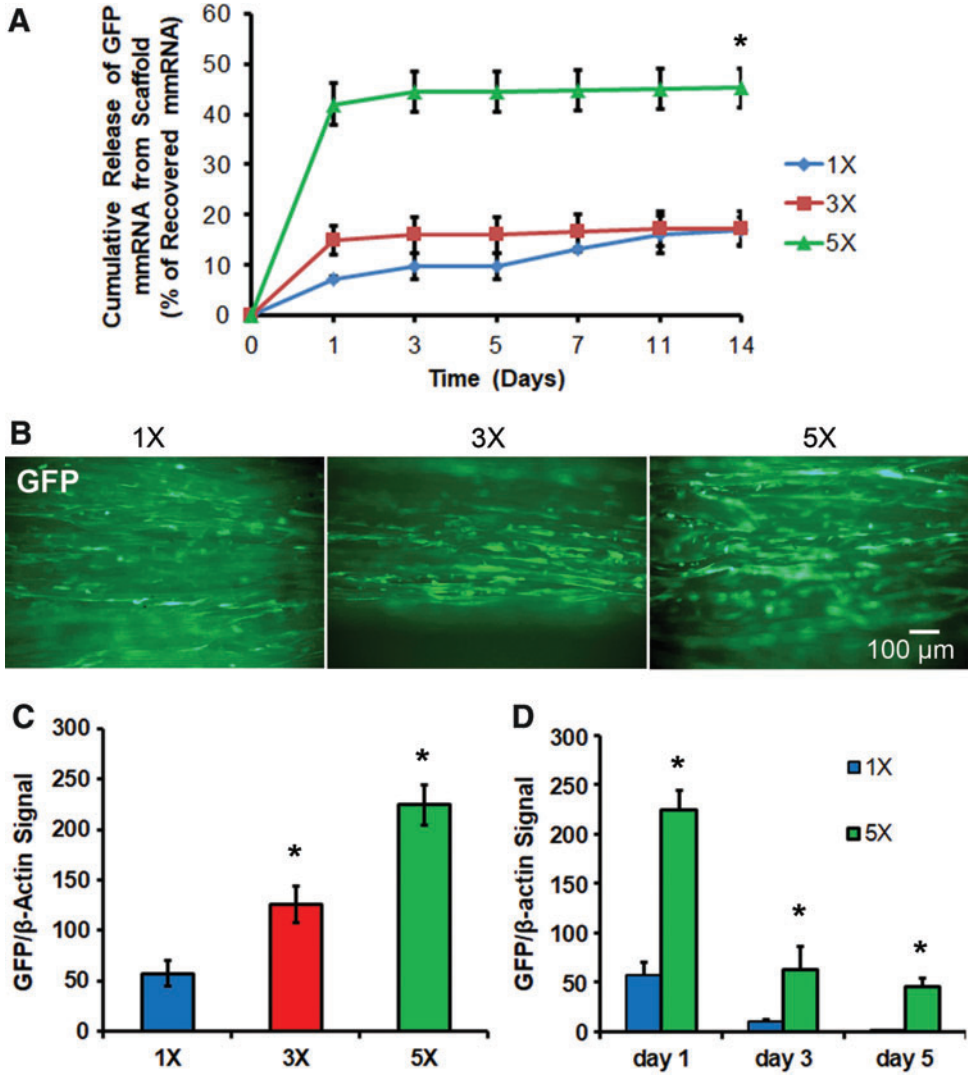

FIG. 3. Characterization of GFP mmRNA release from scaffold and *in vitro* transfection. **(A)** Cumulative mmRNA release from GFP mmRNA-loaded aligned nanofibrillar scaffolds expressed relative to the total recovered mmRNA ($n=3$). Initial mmRNA loadings into scaffolds were 90 ng (1×); 270 ng (3×), or 450 ng (5×), ($n=3$). **(B)** Live fluorescence images of GFP one day after seeding of human fibroblasts on GFP mmRNA-releasing nanofibrillar scaffolds**. (C)** Immunoblot quantification of GFP expression in cell lysates after 1 day of transfection for varying initial loads of mmRNA. Graph shows GFP protein normalized to β-actin ($n=3$). **(D)** Immunoblot quantification of GFP expression time course ($n=3$). *Statistically significant relationship, compared to 1× mmRNA loading at the same time point ($p<0.05$). Scale bar: 100 µm. Color images available online at www.liebertpub.com/tea

been shown that introduction of chemically modified nucleotide analogs into IVT-mRNA (mmRNA), for example, of 5-methylcytidine and pseudouridine, ablates triggering of cellular innate immunity mechanism and thus significantly reduces such mmRNA toxicity through reduction of apoptosis and release of cytokines.[9,43,45] It was as well reported that structural modifications of mRNA with artificial cap analogs, chimeric untranslated regions, constant sufficiently long poly-A tail, and introduction of modified nucleotides into mRNA sequence significantly improve stability of such mmRNA molecules compared to their native mRNA analogs.[46,47]

The current approach, in which mmRNA is delivered in solution, is limited by nonspecific cellular transfection or premature clearance from the target tissue. Using a biomaterials-based delivery approach, we showed that mmRNA release and cellular transfection can be successfully achieved using aligned nanofibrillar scaffolds. The salient findings from this study are as follows: (1) GFP mmRNA incorporated into aligned nanofibrillar collagen scaffolds displayed an initial burst of release during the first day, followed by an incremental release over 14 days, although the total recovered mmRNA suggests partial degradation of the mmRNA (Fig. 3A); (2) human fibroblasts could be transfected with mmRNA-releasing scaffolds with as little as 90 ng of GFP mmRNA (Fig. 3B); (3) the efficiency and persistence of transfection correlated with the dose of mmRNA loaded into the scaffold (Fig. 3C, D); (4) Fluc mmRNA transfection could be detected intramuscularly for at least 7 days based on bioluminescence imaging (Fig. 5 and 6); (5) cellular transfection using HGF mmRNA-releasing scaffolds exemplified therapeutic relevance of this scaffold-based mmRNA delivery approach (Fig. 4), and finally, (6) increased capillary density after intramuscular implantation of HGF mmRNA-releasing scaffolds verified angiogenic efficiency of this scaffold-based mmRNA delivery approach (Fig. 7).

The mmRNA appeared to have undergone partial degradation in the aligned collagen scaffolds. The potential reasons could be due to the stability of mmRNA in the presence of naturally derived biomaterials such as purified collagen, which could contain trace amounts of RNAses or other enzymes. Another contributing factor to the degradation of mmRNA could be the negative pressure associated with the freeze drying step for incorporating mmRNA into the scaffold. As the use of mmRNA is relatively recent, there is limited knowledge of the stability of mmRNA when subjected to harsh temperature and pressure changes associated

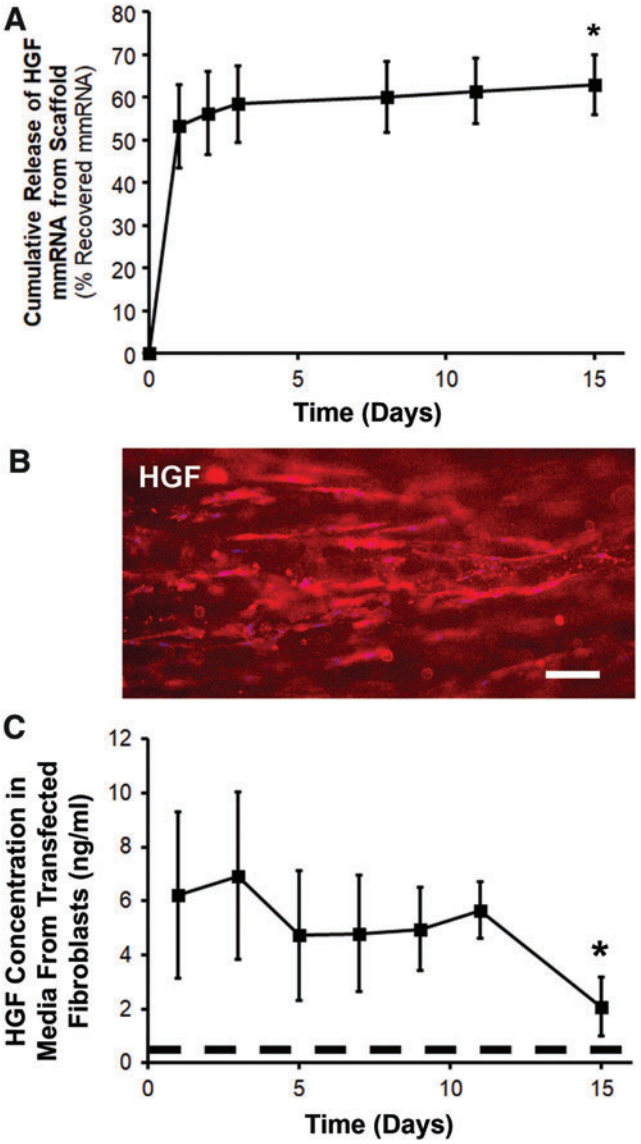

FIG. 4. Characterization of HGF mmRNA release from scaffold and *in vitro* transfection. HGF mmRNA (450 ng, 5×) was loaded into scaffolds. **(A)** Cumulative mmRNA release from HGF mmRNA-loaded aligned nanofibrillar scaffold expressed relative to the total recovered mmRNA ($n=3$). **(B)** HGF-positive cells on HGF-mmRNA scaffold, 1 day after seeding. **(C)** HGF concentration in media from fibroblasts cultured on HGF mRNA-loaded scaffold quantified by HGF ELISA ($n=4$). *Dotted line* denotes the highest detectable level of endogenous HGF in control samples. *Statistically significant relationship, compared to day 0 ($p<0.05$). Scale bar: 100 μm. Color images available online at www.liebertpub.com/tea

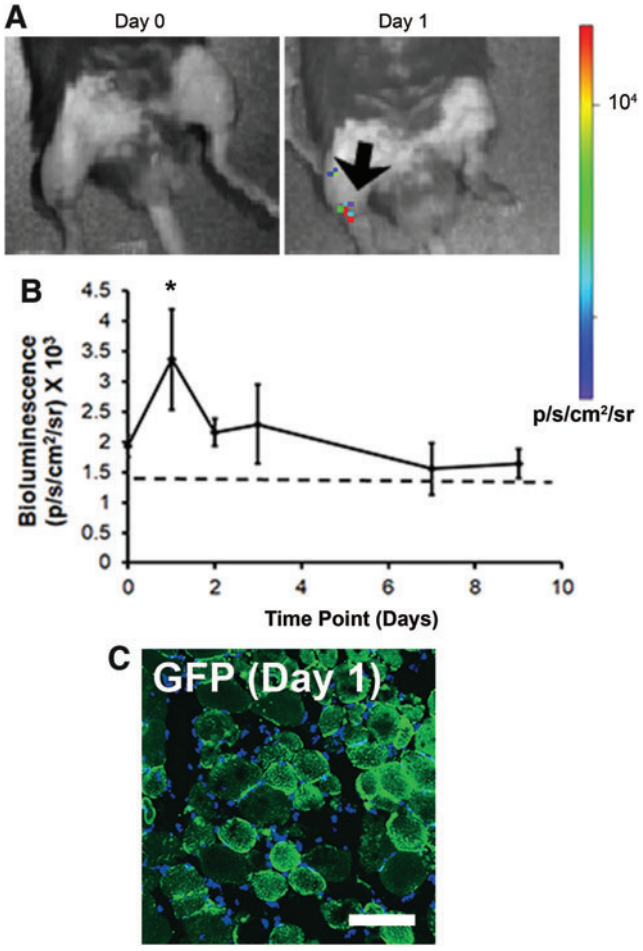

FIG. 5. *In vivo* transfection with Fluc mmRNA-releasing scaffolds after intramuscular implantation in mice. Scaffolds were implanted to the TA muscle after a partial thickness incision. **(A)** Bioluminescence images show Fluc signal localized to the murine TA muscle, showing peak signal on day 1 (*arrow*). Initial mmRNA loading was 20 μg. **(B)** Time course of Fluc transfection over 9 days ($n=4$). **(C)** GFP signal from intramuscularly implanted scaffold releasing GFP mmRNA after 1 day of implantation. *Dotted line* denotes threshold for a positive signal. *Statistically significant relationship, compared to day 0 ($p<0.05$). Scale bar: 100 μm. Fluc, firefly luciferase; TA, tibialis anterior. Color images available online at www.liebertpub.com/tea

with freeze drying. The greater release of HGF mmRNA, compared with GFP mmRNA, could be due to the differences in nucleotide compositions and coding sequence length between the two mmRNAs, with both factors possibly affecting the rate of mmRNA degradation, optimal conditions for the complexation with lipofectamine (mmRNA: Lipofectamine Ratio), and dynamics of the complex interaction with the tube surface during the release procedure. Although the conditions used resulted in a stable transfection for both GFP and HGF mmRNA, further optimization would benefit therapeutic efficacy of HGF mmRNA.

Despite partial degradation of the mmRNA in the nanofibrillar scaffolds, the mmRNA could successfully transfect cells both *in vitro* and *in vivo*. Our studies suggest that loading of 20 μg of Fluc mmRNA was sufficient for observing a signal as early as 3 h after implantation, with a peak signal after 1 day. Similar findings were also reported by Sultana *et al.*[11] who demonstrated that maximal intracardiac bioluminescence signal on day 1 in the myocardium when injected with 100 μg mmRNA in sucrose citrate buffer.

Compared to conventional systemic delivery approaches, mmRNA release from scaffold enables localized delivery of the transcript at higher concentration, and thus, a lower amount of mRNA might be required to exert therapeutic

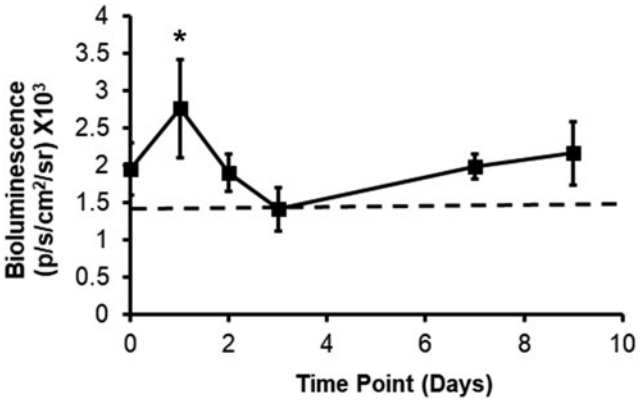

FIG. 6. Bioluminescence imaging depicts *in vivo* transfection with Fluc mmRNA-releasing scaffolds transplanted into a mouse traumatic muscle injury model. Scaffolds were implanted into the void space of the TA muscle after 20% ablation of the muscle. Time course of Fluc transfection over 9 days ($n=4$). *Dotted line* denotes threshold for a positive signal. *Statistically significant relationship, compared to day 0 ($p<0.05$).

effect in the target tissue. The duration of the expression of regenerative factors is another critical parameter in developing mature tissues. Incorporation of mRNA complexes into the scaffold may enable controlled release of the bioactive molecule at the implantation site, which potentially maintains the protein expression at the therapeutic level.[48] The sustained yet temporal release of mRNA transcript can

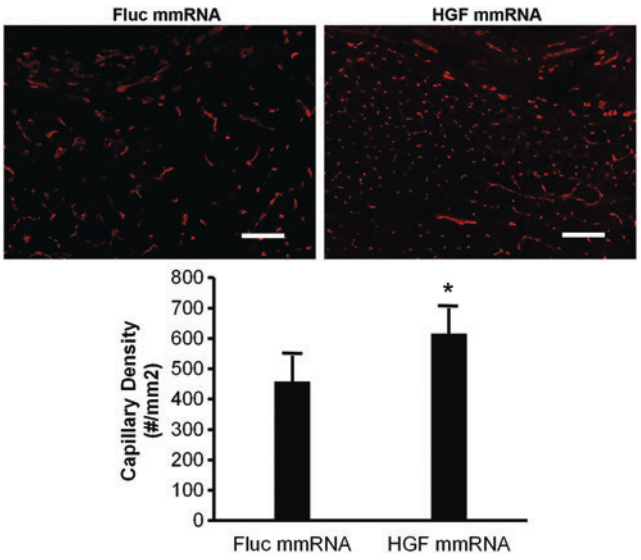

FIG. 7. Therapeutic effect of HGF mmRNA-loaded scaffolds on vascular regeneration of traumatically injured muscle. Immunofluorescence analysis of angiogenesis by treatment of HGF mmRNA-releasing scaffolds, compared to control Fluc mmRNA-releasing scaffolds, at 2 weeks after muscle injury by 20% ablation of the TA muscle in mice. Capillary density was quantified based on CD31 expression adjacent to the site of implanted scaffold. Data are presented as mean ± standard deviation ($n=4$). *Statistically significant relationship, compared to day 0 ($p<0.05$). Scale bar: 100 μm. Color images available online at www.liebertpub.com/tea

also prevent inappropriately high expression of the encoding protein, resulting in lower risk of abnormal tissue formation reported for DNA vectors.[49]

The morphology and physicochemical properties of the scaffold play a significant role in determining transfection efficiency of mRNA, through regulating transcript stability, endocytosis, and cell trafficking.[50] Natural tissue development is a complicated process that requires spatially and temporally patterned expression of different types of proteins, signaling molecules, and matrix molecules in the cellular environment. mRNA incorporation into the aligned scaffold may recreate the spatial patterns in encoded protein expression by the oriented cells attached to the scaffold, which can potentially direct the tissue formation and development of spatially patterned structures such as blood vessels.[48,51]

Postfabrication nonspecific adsorption of mRNA to the scaffold not only minimizes the risk of mRNA degradation during the fabrication/encapsulation process but also locates the mRNA near/on the surface of the scaffold, which may facilitate the cellular uptake by the cells attached to the substrate. The increased surface area and three-dimensional porous structure of the nanofibrillar scaffold may also contribute to uniform distribution of mRNA complexes throughout the scaffold. The scaffold material is another key factor in developing functional gene-activated constructs. As an exogenous material, the scaffold may trigger inflammatory responses. The use of collagen as one of the main components of natural ECM can minimize the inflammatory responses, and subsequently reduce mRNA degradation and elimination of the transfected cells [52]. Moreover, the scaffold material can modulate transfection efficiency not only through regulating cell adhesion and subsequent transfection but also by determining the cell internalization pathway of the gene complex [53].

Having shown a therapeutic effect of HGF-mmRNA-releasing scaffold in a clinically relevant injury model, we envision that scaffold-based delivery of mmRNA may be applied for treatment of a variety of diseases, including those of the cardiovascular, nervous, and musculoskeletal systems. For example, for treatment of peripheral arterial disease that is characterized by vascular obstructions in the limbs, the scaffold loaded with mmRNA-encoding angiogenic factors could be transplanted to the skeletal muscle adjacent to the vascular obstruction to allow for transient growth factor delivery to augment neovascularization. The findings from this work have important implications for the design of gene therapy for soft tissue regeneration.

Conclusion

In summary, we demonstrated that aligned nanofibrillar scaffolds are a potent vehicle for cellular transfection using mmRNA. The scaffolds released mmRNA in a transient and temporally controlled manner. When the scaffolds were cultured with human fibroblasts *in vitro*, cellular transfection could be observed for at least 5 days, and the transfection efficiency correlated with the amount of loaded mmRNA. Furthermore, scaffold-based delivery of mmRNA into injured skeletal muscle resulted in localized cellular transfection, and the angiogenic effect of scaffold-based HGF mmRNA release could be observed at 14 days after transplantation. The long-term impact of scaffold-based mmRNA

delivery technology is an off-the-shelf form of gene therapy for human patients affected by a broad range of diseases or injuries.

Acknowledgments

This work is supported, in part, by the U.S. Army Medical Research and Materiel Command (W81XWH-16-C-0009 to M.V.P.), the Alliance for Regenerative Rehabilitation Research and Training (to N.F.H.), and the National Institutes of Health (P2CHD086843). We thank Drs. Thomas A. Rando, MD, PhD, and Marco Quarta, PhD, for technical assistance with animal studies. We are grateful to Drs. Alex Groisman, Edgar Gutierrez, and Eugene Tkachenko (MuWells) for the fabrication of custom-made plates with aligned collagen coating. The views, opinions, and/or findings contained in this report are those of the author(s) and should not be construed as an official Department of the Army position, policy or decision.

Disclosure Statement

No competing financial interests exist.

References

1. Pahle, J., and Walther, W. Vectors and strategies for nonviral cancer gene therapy. Expert Opin Biol Ther **16,** 443, 2016.
2. Seidlits, S.K., Gower, R.M., Shepard, J.A., and Shea, L.D. Hydrogels for lentiviral gene delivery. Expert Opin Drug Deliv **10,** 499, 2013.
3. Scholz, C., and Wagner, E. Therapeutic plasmid DNA versus siRNA delivery: common and different tasks for synthetic carriers. J Control Release **161,** 554, 2012.
4. Van Tendeloo, V.F., Ponsaerts, P., and Berneman, Z.N. mRNA-based gene transfer as a tool for gene and cell therapy. Curr Opin Mol Ther **9,** 423, 2007.
5. Kormann, M.S., Hasenpusch, G., Aneja, M.K., *et al*. Expression of therapeutic proteins after delivery of chemically modified mRNA in mice. Nat Biotechnol **29,** 154, 2011.
6. Ramunas, J., Yakubov, E., Brady, J.J., *et al*. Transient delivery of modified mRNA encoding tert rapidly extends telomeres in human cells. FASEB J **29,** 1930, 2015.
7. Wang, Y., Su, H.H., Yang, Y., *et al*. Systemic delivery of modified mRNA encoding herpes simplex virus 1 thymidine kinase for targeted cancer gene therapy. Mol Ther **21,** 358, 2013.
8. Kariko, K., Muramatsu, H., Keller, J.M., and Weissman, D. Increased erythropoiesis in mice injected with submicrogram quantities of pseudouridine-containing mRNA encoding erythropoietin. Mol Ther **20,** 948, 2012.
9. Kariko, K., Muramatsu, H., Welsh, F.A., *et al*. Incorporation of pseudouridine into mRNA yields superior nonimmunogenic vector with increased translational capacity and biological stability. Mol Ther **16,** 1833, 2008.
10. Groth, K., Berezhanskyy, T., Aneja, M.K., *et al*. Tendon healing induced by chemically modified mRNAs. Eur Cells Mater **33,** 294, 2017.
11. Sultana, N., Magadum, A., Hadas, Y., *et al*. Optimizing cardiac delivery of modified mRNA. Mol Ther **25,** 1306, 2017.
12. Andre, F.M., Cournil-Henrionnet, C., Vernerey, D., Opolon, P., and Mir, L.M. Variability of naked DNA expression after direct local injection: the influence of the injection speed. Gene Ther **13,** 1619, 2006.
13. Wolff, J.A., Malone, R.W., Williams, P., *et al*. Direct gene transfer into mouse muscle in vivo. Science **247,** 1465, 1990.
14. Zangi, L., Lui, K.O., von Gise, A., *et al*. Modified mRNA directs the fate of heart progenitor cells and induces vascular regeneration after myocardial infarction. Nat Biotechnol **31,** 898, 2013.
15. Pardi, N., Tuyishime, S., Muramatsu, H., *et al*. Expression kinetics of nucleoside-modified mRNA delivered in lipid nanoparticles to mice by various routes. J Control Release **217,** 345, 2015.
16. Jang, J.H., Rives, C.B., and Shea, L.D. Plasmid delivery in vivo from porous tissue-engineering scaffolds: transgene expression and cellular transfection. Mol Ther **12,** 475, 2005.
17. Holladay, C., Keeney, M., Greiser, U., Murphy, M., O'Brien, T., and Pandit, A. A matrix reservoir for improved control of non-viral gene delivery. J Control Release **136,** 220, 2009.
18. Berry, M., Gonzalez, A.M., Clarke, W., *et al*. Sustained effects of gene-activated matrices after CNS injury. Mol Cell Neurosci **17,** 706, 2001.
19. Balmayor, E.R., Geiger, J.P., Koch, C., *et al*. Modified mRNA for BMP-2 in combination with biomaterials serves as a transcript-activated matrix for effectively inducing osteogenic pathways in stem cells. Stem Cells Dev **26,** 25, 2017.
20. Elangovan, S., Khorsand, B., Do, A.V., *et al*. Chemically modified RNA activated matrices enhance bone regeneration. J Control Release **218,** 22, 2015.
21. Badieyan, Z.S., Berezhanskyy, T., Utzinger, M., *et al*. Transcript-activated collagen matrix as sustained mRNA delivery system for bone regeneration. J Control Release **239,** 137, 2016.
22. Leppanen, P., Kholova, I., Mahonen, A.J., *et al*. Short and long-term effects of hVEGF-A(165) in Cre-activated transgenic mice. PLoS One **1,** e13, 2006.
23. Kim, D.H., Provenzano, P.P., Smith, C.L., and Levchenko, A. Matrix nanotopography as a regulator of cell function. J Cell Biol **197,** 351, 2012.
24. Lai, E.S., Huang, N.F., Cooke, J.P., and Fuller, G.G. Aligned nanofibrillar collagen regulates endothelial organization and migration. Regen Med **7,** 649, 2012.
25. Wu, H., Fan, J., Chu, C.C., and Wu, J. Electrospinning of small diameter 3-D nanofibrous tubular scaffolds with controllable nanofiber orientations for vascular grafts. J Mater Sci Mater Med **21,** 3207, 2010.
26. Ma, Z., He, W., Yong, T., and Ramakrishna, S. Grafting of gelatin on electrospun poly(caprolactone) nanofibers to improve endothelial cell spreading and proliferation and to control cell Orientation. Tissue Eng **11,** 1149, 2005.
27. Huang, N.F., Lai, E.S., Ribeiro, A.J., *et al*. Spatial patterning of endothelium modulates cell morphology, adhesiveness and transcriptional signature. Biomaterials **34,** 2928, 2013.
28. Huang, N.F., Okogbaa, J., Lee, J.C., *et al*. The modulation of endothelial cell morphology, function, and survival using anisotropic nanofibrillar collagen scaffolds. Biomaterials **34,** 4038, 2013.
29. Yang, J., McNamara, L.E., Gadegaard, N., *et al*. Nanotopographical induction of osteogenesis through adhesion, bone morphogenic protein cosignaling, and regulation of microRNAs. ACS Nano **8,** 9941, 2014.
30. Downing, T.L., Soto, J., Morez, C., *et al*. Biophysical regulation of epigenetic state and cell reprogramming. Nat Mater **12,** 1154, 2013.

31. Huang, N.F., Patel, S., Thakar, R.G., *et al*. Myotube assembly on nanofibrous and micropatterned polymers. Nano Lett **6,** 537, 2006.
32. Paukshto, M., Fuller, G., Michailov, A., and Remizov, S. Optics of sheared liquid-crystal polarizer based on aqueous dispersion of dichroic-dye nano-aggregates. J Soc Inf Display **13,** 765, 2005.
33. Ukai, Y., Ohyama, T., Fennell, L., *et al*. 38.1: Invited Paper: Current status and future prospect of in-cell polarizer technology. SID Symposium Digest **35,** 1170, 2004.
34. Kirkwood, J.E., and Fuller, G.G. Liquid crystalline collagen: a self-assembled morphology for the orientation of mammalian cells. Langmuir **25,** 3200, 2009.
35. Paukshto, M., McMurtry, D., Bobrov, Y., and Sabelman, E. Oriented Collagen-Based Materials, Films and Methods of Making Same. World Intellectual Property Organization WO/2008/131293, 2008.
36. Bobrov, Y., Fennell, L., Lazarev, P., Paukshto, M., and Remizov, S. Manufacturing of a thin-film LCD. J Soc Inf Display **10,** 317, 2002.
37. Muthusubramaniam, L., Peng, L., Zaitseva, T., Paukshto, M., Martin, G.R., and Desai, T.A. Collagen fibril diameter and alignment promote the quiescent keratocyte phenotype. J Biomed Mater Res A **100,** 613, 2012.
38. McMurtry, D., Paukshto, M., and Bobrov, Y. A Liquid Film Applicator Assembly and Rectilinear Shearing System Incorporating the Same. World Intellectual Property Organization WO/2008/063631, 2008.
39. Paukshto, M.V., McMurtry, D.H., Martin, G.R., Zaitseva, T., and Bobrov, Y.A. Biocomposites and Methods of Making the Same. World Intellectual Property Organization WO/2010/019625, 2010.
40. Nakayama, K.H., Hong, G., Lee, J.C., *et al*. Aligned-braided nanofibrillar scaffold with endothelial cells enhances arteriogenesis. ACS Nano **9,** 6900, 2015.
41. Quarta, M., Cromie, M., Chacon, R., *et al*. Bioengineered constructs combined with exercise enhance stem cell-mediated treatment of volumetric muscle loss. Nat Commun **8,** 15613, 2017.
42. Huang, N.F., Niiyama, H., Peter, C., *et al*. Embryonic stem cell-derived endothelial cells engraft into the ischemic hindlimb and restore perfusion. Arterioscler Thromb Vasc Biol **30,** 984, 2010.
43. Kariko, K., Buckstein, M., Ni, H., and Weissman, D. Suppression of RNA recognition by Toll-like receptors: the impact of nucleoside modification and the evolutionary origin of RNA. Immunity **23,** 165, 2005.
44. Transfection Efficiency of Modified vs. Unmodified mRNA, MTI GlobalStem, 2015. Available at www.mti-globalstem.com/image/catalog/Application/Transfection%20efficiency%20of%20modified%20vs%20unmodified%20mRNA.pdf (accessed June 8, 2018).
45. Heil, F., Hemmi, H., Hochrein, H., *et al*. Species-specific recognition of single-stranded RNA via toll-like receptor 7 and 8. Science **303,** 1526, 2004.
46. Michiels, A., Tuyaerts, S., Bonehill, A., *et al*. Electroporation of immature and mature dendritic cells: implications for dendritic cell-based vaccines. Gene Ther **12,** 772, 2005.
47. Holtkamp, S., Kreiter, S., Selmi, A., *et al*. Modification of antigen-encoding RNA increases stability, translational efficacy, and T-cell stimulatory capacity of dendritic cells. Blood **108,** 4009, 2006.
48. Houchin-Ray, T., Swift, L.A., Jang, J.H., and Shea, L.D. Patterned PLG substrates for localized DNA delivery and directed neurite extension. Biomaterials **28,** 2603, 2007.
49. De Laporte, L., and Shea, L.D. Matrices and scaffolds for DNA delivery in tissue engineering. Adv Drug Deliv Rev **59,** 292, 2007.
50. Jang, J.H., Bengali, Z., Houchin, T.L., and Shea, L.D. Surface adsorption of DNA to tissue engineering scaffolds for efficient gene delivery. J Biomed Mater Res A **77,** 50, 2006.
51. Carlson, B.M. Human Embryology and Developmental Biology, 2nd ed. St Louis: Mosby, 1999.
52. Kao, W.J. Evaluation of protein-modulated macrophage behavior on biomaterials: designing biomimetic materials for cellular engineering. Biomaterials **20,** 2213, 1999.
53. Bengali, Z., Rea, J.C., and Shea, L.D. Gene expression and internalization following vector adsorption to immobilized proteins: dependence on protein identity and density. J Gene Med **9,** 668, 2007.

Address correspondence to:
Ngan F. Huang, PhD
Department of Cardiothoracic Surgery
Stanford University
300 Pasteur Drive, MC 5407
Stanford, CA 94305-5407

E-mail: ngantina@stanford.edu

Received: November 29, 2017
Accepted: April 26, 2018
Online Publication Date: June 15, 2018